

Superconvergence analysis of linear FEM based on polynomial preserving recovery for Helmholtz equation with high wave number

Yu Du^{a,c,*}, Haijun Wu^b, Zhimin Zhang^{a,d}

^a Beijing computational science research center, Beijing, 100193, China

^b Department of Mathematics, Nanjing University, Jiangsu, 210093, China

^c Department of Mathematics, Xiangtan University, Hunan, 411105, China

^d Department of Mathematics, Wayne State University, Detroit, MI 48202, United States of America



ARTICLE INFO

Article history:

Received 25 April 2019

Received in revised form 28 November 2019

MSC:

65N15

76D07

65N30

Keywords:

Helmholtz equation

Large wave number

Pollution errors

Superconvergence

Polynomial preserving recovery

Finite element methods

ABSTRACT

Although superconvergence properties of the polynomial preserving recovery (PPR) for finite element methods (FEM) for coercive elliptic problems are well-understood, the superconvergence behavior of PPR for the Helmholtz equation with high wave number still remains unclear. We study the superconvergence property of the linear FEM with PPR for the two dimensional Helmholtz equation on triangulations satisfying the $O(h^{1+\alpha})$ approximate parallelogram property for some constant $\alpha > 0$. We prove the supercloseness on the H^1 -seminorm between the finite element solution and the linear interpolant of the exact solution under $k(kh)^2 \leq C_0$, where k is the wave number and h is the mesh size. Then, we obtain the superconvergence result based on the PPR technique which says that the PPR improves only the interpolation error but keeps the pollution error unchanged. Finally, we provide numerical tests to verify the superconvergence property and to demonstrate that the PPR combining with the continuous interior penalty technique is much effective for improving both the interpolation error and the pollution error.

© 2020 Elsevier B.V. All rights reserved.

1. Introduction

Let $\Omega \in \mathbb{R}^2$ be a bounded convex polygon with boundary $\Gamma := \partial\Omega$. We consider the Helmholtz problem:

$$-\Delta u - k^2 u = f \quad \text{in } \Omega, \quad (1.1)$$

$$\frac{\partial u}{\partial n} + \mathbf{i}ku = g \quad \text{on } \Gamma, \quad (1.2)$$

where $\mathbf{i} = \sqrt{-1}$ denotes the imaginary unit and n denotes the unit outward normal to Γ . The above Helmholtz problem is an approximation of the following acoustic scattering problem (with time dependence $e^{\mathbf{i}\omega t}$):

$$-\Delta u - k^2 u = f \quad \text{in } \mathbb{R}^2, \quad (1.3)$$

$$\sqrt{r} \left(\frac{\partial(u - u^{\text{inc}})}{\partial r} + \mathbf{i}k(u - u^{\text{inc}}) \right) \rightarrow 0 \quad \text{as } r = |x| \rightarrow \infty, \quad (1.4)$$

* Corresponding author at: Beijing computational science research center, Beijing, 100193, China.

E-mail addresses: duyu@xtu.edu.cn (Y. Du), hjw@nju.edu.cn (H. Wu), zmzhang@csrc.ac.cn, ag7761@wayne.edu (Z. Zhang).

where u^{inc} is the incident wave and k is known as the wave number. The Robin boundary condition (1.2) is known as the first order approximation of the radiation condition (1.4) (cf. [1]). We remark that the Helmholtz problem (1.1)–(1.2) also arises in applications as a consequence of frequency domain treatment of attenuated scalar waves (cf. [2]).

It is well-known that the finite element method (FEM) of fixed order for the Helmholtz problem (1.1)–(1.2) at high frequencies ($k \gg 1$) is subject to the effect of pollution: the ratio of the error of the finite element solution to the error of the best approximation from the finite element space cannot be uniformly bounded with respect to k (see [3–5]). More precisely, the linear finite element method for a 2-D Helmholtz problem satisfies the following error estimate under the mesh constraint $k(kh)^2 \leq C_0$ (cf. [6,7]):

$$\|\nabla u - \nabla u_h\|_{L^2(\Omega)} \leq C_1 kh + C_2 k(kh)^2. \quad (1.5)$$

Here u_h is the linear finite element solution, h is the mesh size and C_i , $i = 1, 2$ are positive constants independent of k and h . It is easy to see that the order of the first term on the right hand side of (1.5) is the same to that of the interpolation error in H^1 -seminorm and it can dominate the error bound only if $k(kh)$ is small enough. However, the second term on the right-hand side of (1.5) dominates the estimate under other mesh conditions. For example, kh is fixed and k is large enough. The term $C_2 k(kh)^2$ is called the pollution error of the finite element solution (see [4,7,8]).

Considerable efforts have been made in analysis of different numerical methods for the Helmholtz problem with large wave number in the literature. The readers are referred to [2,9,10] for asymptotic error estimates of general DG methods and [8,11] for pre-asymptotic error estimates of a one-dimensional problem discretized on equidistant grid. For more pre-asymptotic error estimates, Please refer to [12,13] and [6,14] for classical finite element methods as well as interior penalty finite element methods. For other methods solving Helmholtz problems, such as the interior penalty discontinuous Galerkin method and the source transfer domain decomposition method, one can read [15–18].

In this work, we investigate the superconvergence property of the linear finite element method when being post-processed by the polynomial preserving recovery (PPR) for the Helmholtz problem. The PPR technique was proposed by Zhang and Naga (cf. [19]) and has been successfully applied to finite element methods. COMSOL Multiphysics adopted the PPR as a post-processing tool since 2008 (cf. [20]). One important feature of the PPR is its superconvergence property for the recovered gradient. To learn more about the PPR, readers are referred to [21,22]. Some theoretical results about recovery techniques and recovery-type error estimators can be found in [23–25].

The major purpose of this paper is to analyze the wave number explicit superconvergent estimate of the finite element solution being post-processed by PPR. First we prove the supercloseness between the finite element solution u_h and the interpolant u_I under the assumption that the triangulation \mathcal{T}_h of Ω satisfies the $O(h^{1+\alpha})$ approximate parallelogram property for some constant $\alpha > 0$ (see (2.5) and Definition 2.1). Then based on the superclose estimate, we obtain the following superconvergence of the PPR gradient $G_h u_h$,

$$\|\nabla u - G_h u_h\|_{L^2(\Omega)} \lesssim kh^{1+\alpha} + (kh)^2 |\log h|^{\frac{1}{2}} + k(kh)^2 \quad (1.6)$$

under the condition $k(kh)^2 \leq C_0$, where C_0 is a constant independent of k and h . Comparing with the preasymptotic error estimate of the FE solution (1.5), it seems that the PPR improves the interpolation error from $O(kh)$ to $O(kh^{1+\alpha} + (kh)^2 |\log h|^{\frac{1}{2}})$ but still suffers from the pollution error $O(k^3 h^2)$. To prove that the result (1.6) is not an overestimate, we further analyze the influence of the PPR method on the pollution errors and obtain

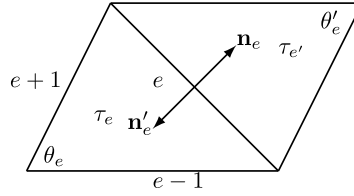
$$\|G_h u_h - \nabla u_h\|_{L^2(\Omega)} \lesssim kh,$$

which means that the pollution term in (1.6) cannot be dropped and that $\|G_h u_h - \nabla u_h\|_{L^2(\Omega)}$ is a good estimator of the error $\|\nabla u - \nabla u_h\|_{L^2(\Omega)}$ only if $k^2 h \lesssim 1$. As a matter of fact, we show that $\|G_h u_h - \nabla u_h\|_{L^2(\Omega)}$ is actually superclose to $\|\nabla u - \nabla P_h u\|_{L^2(\Omega)}$ where $P_h \cdot$ is an elliptic projection operator given by (2.7).

The continuous interior penalty (CIP) technique was first applied to FEM for elliptic and parabolic problems (cf. [26]) and then applied to FEM for Helmholtz equations with high wave number to reduce significantly the pollution error (see [7,14]). This motivates us to combine the PPR with the CIP technique to improve both the interpolation error and the pollution error. Our extensive numerical tests show that the PPR combining with the CIP technique does improve the numerical solution effectively and provide recovered gradients with impressive superconvergence properties not only on “good” quasi-uniform meshes but also on local refined meshes generated by the adaptive algorithm.

The remainder of this paper is organized as follows. Some notation, the linear FEM, and the mesh constraints are introduced in Section 2. In Section 3, we prove the supercloseness between the linear interpolant of the exact solution and the finite element solution. In Section 4, we prove the superconvergence of the recovered gradient of the linear FE solution based on the PPR method, discuss the influence of the PPR technique on the pollution error, and introduce the CIPFEM. Finally, we provide numerical examples to illustrate the performance of the PPR.

Throughout the paper, denote by C a generic positive constant which is independent of h , k , f and g . We also use the shorthand notation $A \lesssim B$ and $A \gtrsim B$ for the inequality $A \leq CB$ and $A \geq B$. $A \approx B$ is a shorthand notation for the statement $A \lesssim B$ and $B \lesssim A$. We assume that $k \gg 1$ since we are considering high-frequency problems and that k is constant on Ω for ease of presentation.

Fig. 1. Notation in the patch Ω_e .

2. Preliminaries

2.1. The linear FEM

Denote by \mathcal{T}_h the regular triangulation of Ω . \mathcal{E}_h is the set of all edges of \mathcal{T}_h and \mathcal{N}_h is the set of all nodal points. For any $\tau \in \mathcal{T}_h$, denote by h_τ its diameter and by $|\tau|$ its area. Define $h_e := \text{diam}(e)$ for $e \in \mathcal{E}_h$. Let $h = \max_{\tau \in \mathcal{T}_h} h_\tau$. Throughout the paper, we assume that $h_\tau \approx h$. We decompose \mathcal{E}_h into two parts \mathcal{E}_h^I and \mathcal{E}_h^B , where $\mathcal{E}_h^B := \{e \in \mathcal{E}_h : e \subset \Gamma\}$ and $\mathcal{E}_h^I := \mathcal{E}_h \setminus \mathcal{E}_h^B$.

Let V_h be the approximation space of continuous piecewise linear polynomials,

$$V_h := \{v_h \in H^1(\Omega) : v_h|_\tau \in P_1(\tau) \forall \tau \in \mathcal{T}_h\},$$

where $P_1(\tau)$ is the set of all polynomials on τ with degree ≤ 1 .

The variational problem to (1.1)–(1.2) reads as follows: Find $u \in H^1(\Omega)$ such that

$$a(u, v) = (f, v) + \langle g, v \rangle \quad \forall v \in H^1(\Omega), \quad (2.1)$$

where

$$a(u, v) := (\nabla u, \nabla v) + ik \langle u, v \rangle - k^2(u, v) \quad \forall u, v \in H^1(\Omega). \quad (2.2)$$

Then the finite element solution $u_h \in V_h$ satisfies

$$a(u_h, v_h) = (f, v_h) + \langle g, v_h \rangle \quad \forall v_h \in V_h. \quad (2.3)$$

We define the “energy” norm on $H^1(\Omega)$

$$\|v\| := (\|\nabla v\|_0^2 + k^2 \|v\|_0^2)^{\frac{1}{2}} \quad \forall v \in H^1(\Omega), \quad (2.4)$$

which will be often used in the subsequent analysis.

The following lemma is proved in [6,7].

Lemma 2.1. For u and u_h , the solutions to (1.1)–(1.2) and (2.3), there exists a constant C_0 independent of k and h such that if $k(kh)^2 \leq C_0$, then the following error estimates hold,

$$\|u - u_h\| \lesssim (kh + k(kh)^2) \frac{|u|_2}{k}, \quad k \|u - u_h\|_0 \lesssim ((kh)^2 + k(kh)^2) \frac{|u|_2}{k}.$$

2.2. The mesh condition

We now introduce some definitions regarding meshes. For $e \in \mathcal{E}_h^I$, denote by $\Omega_e = \tau_e \cup \tau'_e$ the patch formed by the two elements τ_e and τ'_e sharing e (see Figs. 1–2). For $e \in \mathcal{E}_h$ and the element $\tau_e \in \mathcal{T}_h$ including e , denote by θ_e the angle opposite of the edge e in τ_e , \mathbf{t}_e the unit tangent vector of e with counterclockwise orientation and denote by \mathbf{n}_e the unit outward normal vector of e . h_e, h_{e+1} , and h_{e-1} are the lengths of the three edges of τ_e . Here the subscript $e+1$ or $e-1$ is for orientation. Note that all triangles in \mathcal{T}_h are orientated counterclockwise, and the index $'$ is added for the corresponding quantities in τ' with $\mathbf{t}_e = -\mathbf{t}'_e$ and $\mathbf{n}_e = -\mathbf{n}'_e$ due to the orientation.

For an interior edge $e \in \mathcal{E}_h$, recall that Ω_e , the patch of e , consists of two adjacent triangles sharing e . We say that Ω_e is an approximate parallelogram if the lengths of any two opposite edges differ by at most ϵ , that is

$$|h_{e-1} - h'_{e-1}| + |h_{e+1} - h'_{e+1}| \leq \epsilon. \quad (2.5)$$

We assume that the triangulations satisfy the following $O(h^{1+\alpha})$ approximate parallelogram property (see [22,24,27]) as the superconvergence analysis for coercive elliptic problems with Dirichlet boundary conditions does.

Definition 2.1. The triangulation \mathcal{T}_h is said to satisfy Condition (α) if there exists a constant $\alpha \geq 0$ such that the patch Ω_e is an $O(h^{1+\alpha})$ approximate parallelogram for any interior edge $e \in \mathcal{E}_h^I$.

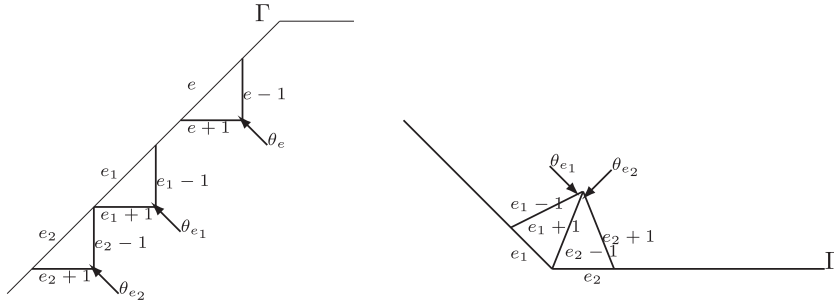


Fig. 2. Notation in the boundary elements.

In order to analyzing the supercloseness for Robin boundary problems, an additional property on element pairs with common boundary nodes is necessary. Denote by \mathcal{N}_h^B the set of all boundary nodes and by \mathcal{N}_h^V the set of all vertices of the polygon Ω . For $z \in \mathcal{N}_h^B$ (cf. Fig. 2), let $e, e' \in \mathcal{E}_h^B$ be the edges sharing z . We say that τ_e and $\tau_{e'}$ are ε approximate congruent triangles if

$$|h_{e-1} - h_{e'-1}| + |h_{e+1} - h_{e'+1}| + |h_e - h_{e'}| \leq \varepsilon. \quad (2.6)$$

Clearly, for an interior edge e , if Ω_e is an ε approximate parallelogram, the two triangles in Ω_e are ε approximate congruent triangles. As a consequence we have the following lemma.

Lemma 2.2. Suppose the triangulation satisfies Condition (α) . Then for $z \in \mathcal{N}_h^B \setminus \mathcal{N}_h^V$ shared by $e, e' \in \mathcal{E}_h^B$ the triangles τ_e and $\tau_{e'}$ are $O(h^{1+\alpha})$ approximate congruent triangles.

We remark that for coercive elliptic problems with Dirichlet boundary conditions superconvergence properties have also be analyzed for some meshes with weaker restrictions than Condition (α) , e.g., the *mildly structured* meshes (cf. [22,28]), in which there may be a small part of interior edges not satisfying the $O(h^{1+\alpha})$ approximate parallelogram property. It is possible to extend the results for the problem with Robin boundary condition in this paper to the mildly structured mesh but with additional $O(h^{1+\alpha})$ approximate congruent restrictions on boundary nodes, since Lemma 2.2 no longer holds. As a matter of fact, we have extended our analysis to coercive elliptic problems with Robin boundary conditions on mildly structured meshes in [29].

2.3. The elliptic projection

Our analysis relies on an elliptic projection $P_h : V \rightarrow V_h$ defined as follows: find $P_h u \in V_h$ such that

$$b(P_h u, v_h) = b(u, v_h) \quad \forall v_h \in V_h. \quad \text{where } b(u, v) := (\nabla u, \nabla v) + \mathbf{i}k \langle u, v \rangle. \quad (2.7)$$

In other words, the elliptic projection $P_h u$ of u is the finite element approximation to the solution of the following (complex-valued) Poisson problem:

$$-\Delta u = F \quad \text{in } \Omega, \quad (2.8)$$

$$\frac{\partial u}{\partial n} + \mathbf{i}ku = g \quad \text{on } \Gamma, \quad (2.9)$$

for some given function F which are determined by u . This kind of elliptic projection is often used to study some properties, such as stability and convergence, of the FEM for the Helmholtz problem (cf. [7,30]).

Lemma 2.3. Assume that u is H^2 -regular. $P_h u$ is its elliptic projection defined by (2.7). There hold the following estimates:

$$\|u - P_h u\| \lesssim (kh + (kh)^2) \frac{|u|_2}{k}, \quad \|u - P_h u\|_0 \lesssim h(kh + (kh)^2) \frac{|u|_2}{k}. \quad (2.10)$$

Proof. From Lemma 3.5 in [6],

$$\begin{aligned} \|u - P_h u\|_1 &\lesssim \inf_{v_h \in V_h} \left(\|u - v_h\|_1^2 + k \|u - v_h\|_{L^2(\Gamma)}^2 \right)^{1/2}, \\ \|u - P_h u\|_0 &\lesssim h \inf_{v_h \in V_h} \left(\|u - v_h\|_1^2 + k \|u - v_h\|_{L^2(\Gamma)}^2 \right)^{1/2}. \end{aligned}$$

On the other hand

$$\begin{aligned} k \|u - v_h\|_{L^2(\Gamma)}^2 &\lesssim k \|u - v_h\|_0 \|u - v_h\|_1 \\ &\lesssim k^2 \|u - v_h\|_0^2 + \|u - v_h\|_1^2 \lesssim \|u - v_h\|^2. \end{aligned}$$

Let $u_I \in V_h$ be the linear interpolant of u . We have

$$\|u - u_I\|_0 + h \|u - u_I\|_1 \lesssim h^2 |u|_2. \quad (2.11)$$

Therefore

$$\|u - P_h u\|_0 + h \|u - P_h u\| \lesssim h \inf_{v_h \in V_h} \|u - v_h\| \lesssim h \|u - u_I\| \lesssim (h^2 + kh^3) |u|_2$$

which completes the proof of the lemma. \square

3. Supercloseness results on the linear interpolant

In this section we derive supercloseness estimates between the linear interpolant u_I of the exact solution u and the FE solution u_h as well as the elliptic projection $P_h u$. Different from most other investigations in the literatures where the Dirichlet boundary condition is considered, the analysis for the Robin boundary condition problems need some more characterization on boundary elements and special arguments.

First we introduce a quadratic interpolant $\psi_Q = \Pi_Q \psi$ of $\psi \in H^2(\tau)$ based on nodal values and moment conditions on edges,

$$(\Pi_Q \phi)(z) = \phi(z), \quad \int_e \Pi_Q \phi = \int_e \phi \quad \forall z \in \mathcal{N}_h, e \in \mathcal{E}_h. \quad (3.1)$$

The following fundamental identity for $v_h \in P_1(\tau)$ has been proved in [27],

$$\int_\tau \nabla(\phi - \phi_I) \cdot \nabla v_h = \sum_{e \in \partial\tau} \left(\beta_e \int_e \frac{\partial^2 \phi_Q}{\partial \mathbf{t}_e^2} \frac{\partial v_h}{\partial \mathbf{t}_e} + \gamma_e \int_e \frac{\partial^2 \phi_Q}{\partial \mathbf{t}_e \partial \mathbf{n}_e} \frac{\partial v_h}{\partial \mathbf{t}_e} \right) \quad (3.2)$$

where

$$\beta_e = \frac{1}{12} \cot \theta_e (h_{e+1}^2 - h_{e-1}^2), \quad \gamma_e = \frac{1}{3} \cot \theta_e |\tau|, \quad (3.3)$$

and $\phi_I \in P_1(\tau)$ is the linear interpolant of ϕ on τ . We have the following technical estimates (see also [27, Lemma 2.13]).

Lemma 3.1. Denote m_e by t_e or n_e . Assume that \mathcal{T}_h satisfies Condition (α) , then we have the following estimates:

(a) For $e \in \mathcal{E}_h^I$,

$$|\beta_e| + |\beta'_e| \lesssim h^2, \quad |\gamma_e| + |\gamma'_e| \lesssim h^2; \quad (3.4)$$

$$|\beta_e - \beta'_e| \lesssim h^{2+\alpha}, \quad |\gamma_e - \gamma'_e| \lesssim h^{2+\alpha}. \quad (3.5)$$

(b) For two adjacent boundary edges $e_1, e_2 \in \mathcal{E}_h^B$ with $e_1 \cap e_2 \in \mathcal{N}_h^B \setminus \mathcal{N}_h^V$,

$$|\beta_{e_1}| + |\beta_{e_2}| \lesssim h^2, \quad |\gamma_{e_1}| + |\gamma_{e_2}| \lesssim h^2; \quad (3.6)$$

$$|\beta_{e_1} - \beta_{e_2}| \lesssim h^{2+\alpha}, \quad |\gamma_{e_1} - \gamma_{e_2}| \lesssim h^{2+\alpha}. \quad (3.7)$$

(c) For $e \in \mathcal{E}_h$, $e \subset \partial\tau_e$,

$$\int_e \frac{\partial^2 \phi}{\partial t_e \partial m_e} \frac{\partial v_h}{\partial t_e} \lesssim (|\phi|_{H^3(\tau_e)} + h^{-1} |\phi|_{H^2(\tau_e)}) \|\nabla v_h\|_{L^2(\tau_e)}; \quad (3.8)$$

$$\int_e \frac{\partial^2(\phi - \phi_Q)}{\partial t_e \partial m_e} \frac{\partial v_h}{\partial t_e} \lesssim |\phi|_{H^3(\tau_e)} \|\nabla v_h\|_{L^2(\tau_e)}. \quad (3.9)$$

Proof. The inequalities (3.4)–(3.6) follow from (3.3) and Condition (α) . (3.7) follows from Definition 2.1, Lemma 2.2 and the law of cosines. (3.8) is using the trace theorem and the scaling argument. (3.9) follows from (3.8) and $|\phi - \phi_Q|_{H^2(\tau_e)} \lesssim h_{\tau_e} |\phi|_{H^3(\tau_e)}$. \square

Lemma 3.2. Assume that \mathcal{T}_h satisfies Condition (α) . Then for $v_h \in V_h$, we have

$$\left| \int_\Omega \nabla(u - u_I) \cdot \nabla v_h \right| \lesssim \left(kh^{1+\alpha} + (kh)^2 |\log h|^{\frac{1}{2}} \right) \|v_h\| C_{u,g}. \quad (3.10)$$

Here u_l is the linear interpolant of u and

$$C_{u,g} = \sum_{j=1}^4 k^{-(j-1)} \|u\|_j + \sum_{j=1}^2 k^{-j} |g|_{H^j(\Gamma)}.$$

Proof. From (3.2), we have

$$\begin{aligned} \int_{\Omega} \nabla(u - u_l) \cdot \nabla v_h &= \sum_{\tau \in \mathcal{T}_h} \sum_{e \subset \partial \tau} \left(\beta_e \int_e \frac{\partial^2 u_Q}{\partial t_e^2} \frac{\partial v_h}{\partial t_e} + \gamma_e \int_e \frac{\partial^2 u_Q}{\partial t_e \partial n_e} \frac{\partial v_h}{\partial t_e} \right) \\ &= I_1 + I_2, \end{aligned}$$

where

$$\begin{aligned} I_1 &= \sum_{e \in \mathcal{E}_h^I} \left[(\beta_e - \beta'_e) \int_e \frac{\partial^2 u}{\partial t_e^2} \frac{\partial v_h}{\partial t_e} + (\gamma_e - \gamma'_e) \int_e \frac{\partial^2 u}{\partial t_e \partial n_e} \frac{\partial v_h}{\partial t_e} \right. \\ &\quad + \beta_e \int_e \frac{\partial^2 (u_Q - u)}{\partial t_e^2} \frac{\partial v_h}{\partial t_e} + \gamma_e \int_e \frac{\partial^2 (u_Q - u)}{\partial t_e \partial n_e} \frac{\partial v_h}{\partial t_e} \\ &\quad \left. + \beta'_e \int_e \frac{\partial^2 (u - u_Q)}{\partial t_e^2} \frac{\partial v_h}{\partial t_e} + \gamma'_e \int_e \frac{\partial^2 (u - u_Q)}{\partial t_e \partial n_e} \frac{\partial v_h}{\partial t_e} \right], \\ I_2 &= \sum_{e \in \mathcal{E}_h^B} \left[\beta_e \int_e \frac{\partial^2 u}{\partial t_e^2} \frac{\partial v_h}{\partial t_e} + \gamma_e \int_e \frac{\partial^2 u}{\partial t_e \partial n_e} \frac{\partial v_h}{\partial t_e} \right. \\ &\quad \left. + \beta_e \int_e \frac{\partial^2 (u_Q - u)}{\partial t_e^2} \frac{\partial v_h}{\partial t_e} + \gamma_e \int_e \frac{\partial^2 (u_Q - u)}{\partial t_e \partial n_e} \frac{\partial v_h}{\partial t_e} \right]. \end{aligned}$$

First, I_1 can be estimated by Lemma 3.1 and the Hölder's inequality:

$$\begin{aligned} |I_1| &\lesssim \sum_{e \in \mathcal{E}_h^I} \left((h^{2+\alpha} + h^2) \|u\|_{H^3(\tau_e)} + h^{1+\alpha} \|u\|_{H^2(\tau_e)} \right) \|\nabla v_h\|_{L^2(\tau_e)} \\ &\lesssim ((h^{2+\alpha} + h^2) \|u\|_3 + h^{1+\alpha} \|u\|_2) \|\nabla v_h\|_0 \\ &\lesssim ((kh)^2 + kh^{1+\alpha}) \|\nabla v_h\|_0 C_{u,g}. \end{aligned} \quad (3.11)$$

We divide I_2 into two parts $I_{2,j} (j = 1, 2)$ to estimate, where

$$I_{2,1} := \sum_{e \in \mathcal{E}_h^B} \left[\beta_e \int_e \frac{\partial^2 (u_Q - u)}{\partial t_e^2} \frac{\partial v_h}{\partial t_e} + \gamma_e \int_e \frac{\partial^2 (u_Q - u)}{\partial t_e \partial n_e} \frac{\partial v_h}{\partial t_e} \right], \quad (3.12)$$

$$I_{2,2} := \sum_{e \in \mathcal{E}_h^B} \left[\beta_e \int_e \frac{\partial^2 u}{\partial t_e^2} \frac{\partial v_h}{\partial t_e} + \gamma_e \int_e \frac{\partial^2 u}{\partial t_e \partial n_e} \frac{\partial v_h}{\partial t_e} \right]. \quad (3.13)$$

From (3.6) and (3.9), we can derive

$$I_{2,1} \lesssim \sum_{e \in \mathcal{E}_h^B} h^2 \|u\|_{H^3(\tau_e)} \|\nabla v_h\|_{L^2(\tau_e)} \lesssim (kh)^2 \|\nabla v_h\|_0 C_{u,g}. \quad (3.14)$$

Then we turn to estimate the remaining contribution $I_{2,2}$. For any boundary node $z \in \mathcal{N}_h^B$, we denote by e_1 and e_2 two boundary edges in \mathcal{E}_h^B sharing z with counterclockwise orientation (cf. Fig. 2). Denote by $[\gamma_e]_z = \gamma_{e_2} - \gamma_{e_1}$. Recall that \mathcal{N}_h^V is the set of vertices of the domain Ω . By integration by parts, We have

$$\begin{aligned} I_{2,2} &= - \sum_{e \in \mathcal{E}_h^B} \left(\beta_e \int_e \frac{\partial^3 u}{\partial t_e^3} v_h + \gamma_e \int_e \frac{\partial^3 u}{\partial^2 t_e^2 \partial n_e} v_h \right) \\ &\quad + \sum_{z \in \mathcal{N}_h^B \setminus \mathcal{N}_h^V} \left([\beta_e]_z \frac{\partial^2 u}{\partial t_e^2}(z) + [\gamma_e]_z \frac{\partial^2 u}{\partial t_e \partial n_e}(z) \right) v_h(z) \\ &\quad + \sum_{z \in \mathcal{N}_h^V} \left(\beta_{e_2} \frac{\partial^2 u}{\partial t_{e_2}^2}(z) - \beta_{e_1} \frac{\partial^2 u}{\partial t_{e_1}^2}(z) + \gamma_{e_2} \frac{\partial^2 u}{\partial t_{e_2} \partial n_{e_2}}(z) - \gamma_{e_1} \frac{\partial^2 u}{\partial t_{e_1} \partial n_{e_1}}(z) \right) v_h(z) \\ &:= I_{2,2,1} + I_{2,2,2} + I_{2,2,3}. \end{aligned}$$

Since $\frac{\partial u}{\partial n} + iku = g$, from (3.6) and the trace theorem, we obtain

$$\begin{aligned} I_{2,2,1} &\lesssim h^2 \left(|u|_{H^3(\Gamma)} + \left| \frac{\partial u}{\partial n} \right|_{H^2(\Gamma)} \right) \|v_h\|_{L^2(\Gamma)} \\ &\lesssim h^2 \left(|u|_{H^3(\Gamma)} + |g|_{H^2(\Gamma)} + k|u|_{H^2(\Gamma)} \right) \cdot \|v_h\|_0^{1/2} \|v_h\|_1^{1/2} \\ &\lesssim k^2 h^2 \|v_h\|_{C_{u,g}}. \end{aligned} \quad (3.15)$$

For any $w \in H^1([a, b])$, there holds

$$\begin{aligned} w^2(b) &= \int_a^b \left(\frac{x-a}{b-a} w^2(x) \right)' dx = \frac{1}{b-a} \int_a^b w^2 + 2 \int_a^b \frac{x-a}{b-a} w w' \\ &\leq \frac{1}{b-a} \|w\|_{L^2([a,b])}^2 + 2 \|w\|_{H^1([a,b])} \|w\|_{L^2([a,b])}, \end{aligned}$$

which together with (3.7) implies

$$\begin{aligned} I_{2,2,2} &\leq \sum_{z \in \mathcal{N}_h^B \setminus \mathcal{N}_h^V} \left(|\beta_e|_z \left(h_e^{-\frac{1}{2}} |u|_{H^2(e)} + h_e^{\frac{1}{2}} |u|_{H^3(e)} \right) \right. \\ &\quad \left. + |\gamma_e|_z \left(h_e^{-\frac{1}{2}} \left| \frac{\partial u}{\partial n_e} \right|_{H^1(e)} + h_e^{\frac{1}{2}} \left| \frac{\partial u}{\partial n_e} \right|_{H^2(e)} \right) \right) \\ &\quad \cdot \left(h_e^{-\frac{1}{2}} \|v_h\|_{L^2(e)} + h_e^{\frac{1}{2}} |v_h|_{H^1(e)} \right) \\ &\lesssim \max_{z \in \mathcal{N}_h^B \setminus \mathcal{N}_h^V} (|\beta_e|_z + |\gamma_e|_z) \left(h^{-\frac{1}{2}} |u|_{H^2(\Gamma)} + h^{\frac{1}{2}} |u|_{H^3(\Gamma)} \right. \\ &\quad \left. + h^{-\frac{1}{2}} \left| \frac{\partial u}{\partial n_e} \right|_{H^1(\Gamma)} + h^{\frac{1}{2}} \left| \frac{\partial u}{\partial n_e} \right|_{H^2(\Gamma)} \right) \cdot h^{-\frac{1}{2}} \|v_h\|_{L^2(\Gamma)} \\ &\lesssim h^{1+\alpha} (|u|_{H^2(\Gamma)} + h|u|_{H^3(\Gamma)} + |g|_{H^1(\Gamma)} + h|g|_{H^2(\Gamma)} \\ &\quad + k|u|_{H^1(\Gamma)} + kh|u|_{H^2(\Gamma)}) \|v_h\|_{L^2(\Gamma)} \\ &\lesssim h^{1+\alpha} (k + k^2 h) \|v_h\|_{C_{u,g}}. \end{aligned} \quad (3.16)$$

Since the number of the vertices of Ω is a bounded constant independent of all the parameters k , h and α , using $\|v_h\|_{L^\infty(\Omega)} \lesssim |\log h|^{\frac{1}{2}} \|v_h\|_{H^1(\Omega)}$ (cf. [31]), we have

$$\begin{aligned} I_{2,2,3} &\lesssim h^2 \max_{z \in \mathcal{N}_h^V} \left(\left| \frac{\partial^2 u}{\partial t_{e_1}^2}(z) \right| + \left| \frac{\partial^2 u}{\partial t_{e_2}^2}(z) \right| \right. \\ &\quad \left. + \left| \frac{\partial^2 u}{\partial t_{e_1} \partial n_{e_1}}(z) \right| + \left| \frac{\partial^2 u}{\partial t_{e_2} \partial n_{e_2}}(z) \right| \right) \|v_h\|_{L^\infty(\Omega)} \\ &\lesssim h^2 \left(|u|_{H^2(\Gamma)} + |u|_{H^2(\Gamma)}^{\frac{1}{2}} |u|_{H^3(\Gamma)}^{\frac{1}{2}} + \|g\|_{H^2(\Gamma)} \right. \\ &\quad \left. + k(|u|_{H^1(\Gamma)} + |u|_{H^1(\Gamma)}^{\frac{1}{2}} |u|_{H^2(\Gamma)}^{\frac{1}{2}}) \right) \cdot |\log h|^{\frac{1}{2}} \|v_h\|_{H^1(\Omega)} \\ &\lesssim k^2 h^2 |\log h|^{\frac{1}{2}} \|v_h\|_{C_{u,g}}. \end{aligned} \quad (3.17)$$

Combining the inequalities (3.15)–(3.17) yields

$$|I_{2,2}| = |I_{2,2,1} + I_{2,2,2} + I_{2,2,3}| \lesssim (kh^{1+\alpha} + k^2 h^2 |\log h|^{\frac{1}{2}}) \|v_h\|_{C_{u,g}}. \quad (3.18)$$

Finally, the proof of the lemma follows by combining (3.11), (3.14), and (3.18). \square

Next, we derive supercloseness estimates of $\|P_h u - u_I\|$ and $\|u_h - u_I\|$. The following lemma gives the supercloseness estimate between the linear interpolant and the elliptic projection.

Lemma 3.3. Assume that \mathcal{T}_h satisfies Condition (α) and u is the exact solution to (1.1)–(1.2). $P_h u$ is its elliptic projection defined by (2.7) and u_I is linear interpolation. We have

$$\|P_h u - u_I\| \lesssim (kh^{1+\alpha} + (kh)^2 |\log h|^{\frac{1}{2}}) C_{u,g}. \quad (3.19)$$

Proof. Denote by $v_h = P_h u - u_I$. By the Galerkin orthogonality,

$$\begin{aligned} \|P_h u - u_I\|^2 &\lesssim \Re((\nabla(P_h u - u_I), \nabla v_h) + ik \langle P_h u - u_I, v_h \rangle) + k^2(P_h u - u_I, v_h) \\ &\lesssim \Re((\nabla(u - u_I), \nabla v_h) + ik \langle u - u_I, v_h \rangle) + k^2(P_h u - u_I, v_h) \\ &\lesssim |(\nabla(u - u_I), \nabla v_h)| + |k \langle u - u_I, v_h \rangle| + k \|P_h u - u_I\|_0 \cdot k \|v_h\|_0. \end{aligned}$$

From Lemma 2.3 and (2.11) we have

$$k \|P_h u - u_I\|_0 \cdot k \|v_h\|_0 \leq (k \|P_h u - u\|_0 + k \|u - u_I\|_0) \|v_h\| \lesssim (kh)^2 \|v_h\| C_{u,g}.$$

On the other hand, by the trace inequality (cf. [32]),

$$\begin{aligned} |k \langle u - u_I, v_h \rangle| &\leq k \|u - u_I\|_{L^2(\partial\Omega)} \|v_h\|_{L^2(\partial\Omega)} \lesssim k^{1/2} h^2 \|u\|_{H^2(\partial\Omega)} \cdot k^{1/2} \|v_h\|_{L^2(\partial\Omega)} \\ &\lesssim k^{1/2} h^2 \|u\|_{H^2(\Omega)}^{1/2} \|u\|_{H^3(\Omega)}^{1/2} \|v_h\| \lesssim (kh)^2 \|v_h\| C_{u,g}. \end{aligned}$$

Then the estimate (3.19) follows by combining Lemma 3.2 and the above three estimates. \square

The error bound in (3.19) consists of two terms. The first term $O(kh^{1+\alpha})$ is the same as the error bound for coercive elliptic problem with Dirichlet boundary condition. The second term $O((kh)^2 |\log h|^{\frac{1}{2}})$ is due to the Robin boundary condition and the corners of the domain Ω .

The following theorem gives the supercloseness estimate between the linear interpolant and the FE solution.

Theorem 3.1. Assume that \mathcal{T}_h satisfies Condition (α) and that $k(kh)^2 \leq C_0$ where C_0 is from Lemma 2.1. Then

$$\|u_h - u_I\| \lesssim (kh^{1+\alpha} + (kh)^2 |\log h|^{\frac{1}{2}} + k(kh)^2) C_{u,g}. \quad (3.20)$$

Proof. Let $\theta_h := u_h - P_h u$. Clearly $u_h - u_I = \theta_h + P_h u - u_I$. From Lemma 3.3, it suffices to show that $\|\theta_h\| \lesssim k^3 h^2 C_{u,g}$. It follows from (2.1)–(2.3) and (2.7) that

$$\begin{aligned} b(\theta_h, \theta_h) &= a(u_h, \theta_h) + k^2(u_h, \theta_h) - b(u, \theta_h) = a(u, \theta_h) + k^2(u_h, \theta_h) - b(u, \theta_h) \\ &= k^2(u_h - u, \theta_h). \end{aligned}$$

By taking the real parts of both sides, we conclude that

$$\|\nabla \theta_h\|_0^2 \lesssim k^2 \|u - u_h\|_0 \|\theta_h\|_0 \lesssim k^2 \|u - u_h\|_0^2 + k^2 \|\theta_h\|_0^2$$

which implies that

$$\|\theta_h\| \lesssim k \|u - u_h\|_0 + k \|\theta_h\|_0 \lesssim k \|u - u_h\|_0 + k \|u - P_h u\|_0 \lesssim k^3 h^2 C_{u,g}$$

where we have used Lemmas 2.1 and 2.3 to derive the last inequality.

This completes the proof. \square

4. Superconvergence based on the PPR

In this section, we apply a gradient recovery operator developed in 2004, called polynomial preserving recovery (PPR) (cf. [19,21]), to improve the finite element solution.

4.1. The PPR operator

We first introduce the gradient recovery operator $G_h : C(\Omega) \mapsto V_h \times V_h$. Given a node $z \in \mathcal{N}_h$, we select $n \geq 6$ sampling points $z_j \in \mathcal{N}_h$, $j = 1, 2, \dots, n$, in an element patch ω_z containing z (z is one of z_j) and fit a polynomial of degree 2, in the least squares sense, with values of u_h at those sampling points. First, we find $p \in P_2(\omega_z)$ for some $w \in C(\Omega)$ such that

$$\sum_{j=1}^n (p - w)^2(z_j) = \min_{q \in P_2} \sum_{j=1}^n (q - w)^2(z_j). \quad (4.1)$$

Here $P_2(\omega_z)$ is the quadratic polynomial space defined on ω_z . Then the recovery gradient at z is then defined as

$$G_h w(z) = (\nabla p)(z). \quad (4.2)$$

For the linear element, the above least squares fitting procedure has a unique solution as long as those n sampling points are not on the same conic curve (cf. [21]).

Now we show some properties of the gradient recovery operator G_h :

- (i) $\|G_h v_h\|_0 \lesssim \|\nabla v_h\|_0 \quad \forall v_h \in V_h$.
- (ii) For any nodal point z , $(G_h p)(z) = \nabla p(z)$ if $p \in P_j(\omega_z)$, $j = 1, 2$.
- (iii) $G_h w = G_h I_h^j w \quad \forall w \in C(\Omega)$, $j = 1, 2$.

Here I_h^j ($j = 1, 2$) are the linear nodal value interpolant and quadratic nodal value interpolant of w , respectively. The reader is referred to [21,22] for more details of these properties.

The following lemma says that the PPR gradient from u itself is superclose to ∇u .

Lemma 4.1. For $\tau \in \mathcal{T}_h$ and $\phi \in H^3(\bar{\tau})$, there holds

$$\|G_h \phi_l - \nabla \phi\|_{L^2(\tau)} \lesssim h^2 |\phi|_{H^3(\bar{\tau})}, \quad (4.3)$$

where $\bar{\tau} = \bigcup \{\omega_z : z \in \mathcal{N}_h \cap \tau\}$ and ϕ_l is the linear interpolant of ϕ .

Proof. By the property (iii), we can obtain

$$\|G_h \phi_l - \nabla \phi\|_{L^2(\tau)} = \|G_h \phi - \nabla \phi\|_{L^2(\tau)} = \|G_h I_h^2 \phi - \nabla \phi\|_{L^2(\tau)}. \quad (4.4)$$

For $\eta \in P_2(\bar{\tau})$, from the property (ii) and the fact that $G_h \eta \in V_h \times V_h$ and $\nabla \eta \in P_1(\bar{\tau}) \times P_1(\bar{\tau})$, thus we have $G_h \eta = \nabla \eta$ in τ , which implies

$$\begin{aligned} \|G_h I_h^2 \phi - \nabla \phi\|_{L^2(\tau)} &= \|G_h(I_h^2 \phi - \eta) - \nabla(\phi - \eta)\|_{L^2(\tau)} \\ &\leq \|G_h(I_h^2 \phi - \eta)\|_{L^2(\tau)} + \|\nabla(\phi - \eta)\|_{L^2(\tau)}. \end{aligned} \quad (4.5)$$

From the definition and properties of G_h , we can obtain a contribution bounded by

$$\begin{aligned} \|G_h(I_h^2 \phi - \eta)\|_{L^2(\tau)} &\lesssim h \max_{z \in \mathcal{N}_h \cap \tau} |G_h(I_h^2 \phi - \eta)(z)| \lesssim h \|\nabla(I_h^2 \phi - \eta)\|_{L^\infty(\bar{\tau})} \\ &\lesssim \|\nabla(I_h^2 \phi - \eta)\|_{L^2(\bar{\tau})} \lesssim \|\nabla(I_h^2 \phi - \phi)\|_{L^2(\bar{\tau})} + \|\nabla(\phi - \eta)\|_{L^2(\bar{\tau})}. \end{aligned} \quad (4.6)$$

Then, from (4.4)–(4.6) we can obtain

$$\|G_h I_h^2 \phi - \nabla \phi\|_{L^2(\tau)} \lesssim \inf_{\eta \in P_2(\bar{\tau})} \|\nabla(\phi - \eta)\|_{L^2(\bar{\tau})} + \|\nabla(I_h^2 \phi - \phi)\|_{L^2(\bar{\tau})}. \quad (4.7)$$

By the Hilbert–Bramble lemma and the scaling argument,

$$\inf_{\eta \in P_2(\bar{\tau})} \|\nabla(\phi - \eta)\|_{L^2(\bar{\tau})} \lesssim h^2 |\phi|_{H^3(\bar{\tau})}, \quad (4.8)$$

and from the approximation theory

$$\|\nabla(I_h^2 \phi - \phi)\|_{L^2(\bar{\tau})} \lesssim h^2 |\phi|_{H^3(\bar{\tau})}. \quad (4.9)$$

The proof is completed by combining (4.4) with (4.7)–(4.9). \square

We remark that there have been many superconvergent results (see [22,33]) for the recovered gradients based on the PPR in recent years. All of them assumed that $u \in H^3(\Omega) \cap W_\infty^2(\Omega)$ instead of $u \in H^3(\Omega)$.

By summing the estimates in Lemma 4.1 over \mathcal{T}_h we have the following theorem.

Theorem 4.1. We have the following estimate:

$$\|G_h u_l - \nabla u\|_0 \lesssim h^2 |u|_3 \lesssim (kh)^2 C_{u,g}. \quad (4.10)$$

Proof. From Lemma 4.1 we have

$$\begin{aligned} \|G_h u_l - \nabla u\|_0 &= \left(\sum_{\tau \in \mathcal{M}_h} \|G_h u_l - \nabla u\|_{L^2(\tau)}^2 \right)^{1/2} \lesssim h^2 \left(\sum_{\tau \in \mathcal{M}_h} |u|_{H^3(\bar{\tau})}^2 \right)^{1/2} \\ &\lesssim h^2 |u|_3 \lesssim (kh)^2 C_{u,g}. \end{aligned}$$

This completes the proof. \square

The above superconvergence result holds for $u \in H^3(\Omega)$. However, if u is only in $H^2(\Omega)$, by following the proofs of Lemma 4.1 and Theorem 4.1 we have

$$\|G_h u_l - \nabla u\|_0 \lesssim h |u|_2. \quad (4.11)$$

4.2. The PPR gradient from the FE solution

The following lemma says that the PPR gradient from the elliptic projection of u is superclose to ∇u .

Lemma 4.2. Assume that \mathcal{T}_h satisfies Condition (α) . Let u be the solution to (1.1)–(1.2). Then

$$\|G_h P_h u - \nabla u\|_0 \lesssim (kh^{1+\alpha} + (kh)^2 |\log h|^{\frac{1}{2}}) C_{u,g}. \quad (4.12)$$

Proof. From (i), we have

$$\begin{aligned} \|G_h P_h u - \nabla u\|_0 &\leq \|G_h P_h u - G_h u_I\| + \|G_h u_I - \nabla u\|_0 \\ &\lesssim \|\nabla(P_h u - u_I)\|_0 + \|G_h u_I - \nabla u\|_0. \end{aligned} \quad (4.13)$$

Then (4.12) follows by combining (4.13), Lemma 3.3 and Theorem 4.1. \square

The following theorem gives a superconvergence estimate between the PPR gradient from u_h and ∇u .

Theorem 4.2. Assume that \mathcal{T}_h satisfies Condition (α) and that $k(kh)^2 \leq C_0$ where C_0 is from Lemma 2.1. Let u and u_h be the solutions to (1.1)–(1.2) and (2.3), respectively. Then

$$\|G_h u_h - \nabla u\|_0 \lesssim (kh^{1+\alpha} + (kh)^2 |\log h|^{\frac{1}{2}} + k(kh)^2) C_{u,g}. \quad (4.14)$$

Proof. Similar to the proof of Lemma 4.2,

$$\|G_h u_h - \nabla u\|_0 \lesssim \|\nabla(u_h - u_I)\|_0 + \|G_h u_I - \nabla u\|_0. \quad (4.15)$$

Then (4.14) follows by combining (4.15), Theorems 3.1 and 4.1. \square

Remark 4.1. From Lemma 2.1 we know that

$$\|\nabla u_h - \nabla u\|_0 \lesssim (kh + k(kh)^2) C_{u,g}. \quad (4.16)$$

It seems that the PPR improves the interpolation error from $O(kh)$ to $O(kh^{1+\alpha} + (kh)^2 |\log h|^{\frac{1}{2}})$ but keeps the pollution error $O(k^3 h^2)$ unchanged. Is it possible that Theorem 4.2 gives an overestimate? The answer is no. Theorem 4.3 and our numerical tests in Section 5 indicate that the pollution error is the same with or without the gradient recovery.

The following theorem gives estimates regarding $\|G_h u_h - \nabla u_h\|_0$.

Theorem 4.3. Assume that $k(kh)^2 \leq C_0$ where C_0 is from Lemma 2.1. Let u_h be the linear finite element solution to the problem (1.1)–(1.2). We have

$$\|G_h u_h - \nabla u_h\|_0 \lesssim h |u|_2. \quad (4.17)$$

If, moreover, \mathcal{T}_h satisfies Condition (α) , the following estimate holds,

$$\begin{aligned} &\left| \|G_h u_h - \nabla u_h\|_0 - \|\nabla u - \nabla P_h u\|_0 \right| \\ &\lesssim (kh^{1+\alpha} + (kh)^2 |\log h|^{\frac{1}{2}} + k^4 h^3) C_{u,g}. \end{aligned} \quad (4.18)$$

Proof. We decompose u_h into $P_h u$ and θ_h where $\theta_h = u_h - P_h u$. Then

$$\begin{aligned} &\|G_h u_h - \nabla u_h - (\nabla u - \nabla P_h u)\|_0 \\ &= \|G_h(P_h u + \theta_h) - \nabla(P_h u + \theta_h) - \nabla u + \nabla P_h u\|_0 \\ &\lesssim \|G_h(P_h u - u_I)\|_0 + \|G_h u_I - \nabla u\|_0 + \|G_h \theta_h - \nabla \theta_h\|_0. \\ &\lesssim \|\nabla(P_h u - u_I)\|_0 + \|G_h u_I - \nabla u\|_0 + \|G_h \theta_h - \nabla \theta_h\|_0. \end{aligned} \quad (4.19)$$

We next estimate the last term in (4.19). From (2.3) and (2.7), θ_h satisfies

$$(\nabla \theta_h, \nabla v_h) + \mathbf{i}k \langle \theta_h, v_h \rangle = -k^2(u - u_h, v_h), \quad \forall v_h \in V_h.$$

Clearly, θ_h can be understood as the finite element solution to the following Poisson problem with Robin boundary:

$$\begin{aligned} -\Delta \theta &= -k^2(u - u_h) \quad \text{in } \Omega, \\ \frac{\partial \theta}{\partial n} + \mathbf{i}k \theta &= 0 \quad \text{on } \Gamma. \end{aligned}$$

That is, $\theta_h = P_h \theta$. It follows from the triangle inequality, (4.11), Lemma 2.3, and the property (i) that

$$\begin{aligned} \|G_h \theta_h - \nabla \theta_h\|_0 &= \|G_h P_h \theta - \nabla P_h \theta\|_0 \\ &\leq \|G_h(P_h \theta - \theta_I)\|_0 + \|G_h \theta_I - \nabla \theta\|_0 + \|\nabla \theta - \nabla P_h \theta\|_0 \\ &\lesssim h \|\theta\|_2 \lesssim k^2 h \|u - u_h\|_0 \lesssim h((kh)^2 + k(kh)^2) |u|_2 \\ &\lesssim (kh)^3 |u|_2 \end{aligned} \quad (4.20)$$

where we have used Lemma 2.1 to derive the second last inequality. Then (4.17) follows by combining (4.19)–(4.20), (4.11), and the assumption $k(kh)^2 \leq C_0$. (4.18) follows by combining (4.19)–(4.20), Theorem 4.1, and Lemma 3.3. This completes the proof of the theorem. \square

Remark 4.2. We have three observations from Theorem 4.3. First, $\|G_h u_h - \nabla u_h\|_0$ is of the same order as the interpolation error. Secondly, noting that $\|G_h u_h - \nabla u\|_0 \geq \|\nabla u_h - \nabla u\|_0 - \|G_h u_h - \nabla u_h\|_0$, (4.17) and Lemma 2.1 imply that the pollution error in $\|\nabla u_h - \nabla u\|_0$ is inherited by $\|G_h u_h - \nabla u\|_0$. Thirdly, unlike the PPR for coercive elliptic problems, $\|G_h u_h - \nabla u_h\|_0$ is not a good estimate of the error $\|\nabla u - \nabla u_h\|_0$ when the pollution error is large. As a consequence of (4.17), $\|G_h u_h - \nabla u_h\|_0$ is actually an asymptotically exact estimate of $\|\nabla u - \nabla P_h u\|_0$.

In summary, The PPR for FEM improves the interpolation error but not the pollution error. In order to improve the pollution error, one approach is to use discretization methods with small pollution error instead of FEM, e.g., the continuous interior penalty FEM as described in the following subsection with appropriate penalty parameters (see also [7,34]).

4.3. Continuous interior penalty finite element method

We shall now introduce the continuous interior penalty FEM (CIP-FEM), that is done by adding some appropriate penalty terms on the jumps of the fluxes across interior edges to the finite element system (2.3).

For every $e = \partial K \cap \partial K' \in \mathcal{E}_h^I$, let n_e be a unit normal vector to e and $[v]$ be the jump of v on e , given by $[v]|_e := v|_{K'} - v|_K$. We define the “energy” space V and the sesquilinear form $a_\gamma(\cdot, \cdot)$ on $V \times V$ as

$$V := H^1(\Omega) \cap \prod_{K \in \mathcal{T}_h} H^2(K),$$

$$a_\gamma(u, v) := a(u, v) + J(u, v) \quad \forall u, v \in V, \quad (4.21)$$

$$J(u, v) := \sum_{e \in \mathcal{E}_h^I} \gamma_e h_e \left\langle \left[\frac{\partial u}{\partial n_e} \right], \left[\frac{\partial v}{\partial n_e} \right] \right\rangle_e, \quad (4.22)$$

where γ_e for $e \in \mathcal{E}_h^I$ are called the penalty parameters, which are complex numbers with nonnegative imaginary parts. It is clear that $J(u, v) = 0$ if $u \in H^2(\Omega)$ and $v \in V$. Therefore, if $u \in H^2(\Omega)$ is the solution to (1.1)–(1.2), then

$$a_\gamma(u, v) = (f, v) + \langle g, v \rangle, \quad \forall v \in V.$$

This motivates the definition of the CIP-FEM: Find $u_h \in V_h$ such that

$$a_\gamma(u_h, v_h) = (f, v_h) + \langle g, v_h \rangle, \quad \forall v_h \in V_h. \quad (4.23)$$

Compared with our earlier standard FEM (2.3), the CIP-FEM (4.23) has added a bilinear form $J(u, v)$ that collects the so-called penalty terms, one from each interior edge of \mathcal{T}_h . Clearly, the CIP-FEM reduces to the standard FEM (2.3) when the penalty parameters γ_e in $J(u, v)$ are turned off.

The CIP-FEM (4.23) was analyzed systematically in [7,34] for the Helmholtz problem (1.1)–(1.2), and shown to be absolutely stable for penalty parameters γ_e with positive imaginary parts. Optimal order preasymptotic error estimates were also derived, and the penalty parameters may be tuned to reduce the pollution errors significantly (see [7,14]). By following the technical derivations and development in Section 4.2, we can establish the superconvergence estimates in Theorem 4.2 and Theorem 4.3 also for the above CIP-FEM. We omit the tedious technical details here.

Remark 4.3. (1) Penalizing the jumps of normal derivatives across interior edges of a finite element mesh was used by Douglas and Dupont (cf. [26]) for second order PDEs, by Babuška and Zlámal (cf. [35]) for the fourth order PDEs in the context of C^0 finite element methods, by Baker (cf. [36]) for the fourth order PDEs and by Arnold (cf. [37]) for second order parabolic PDEs in the context of IPDG methods.

(2) We have considered in this work the scattering problem of the time dependence $e^{i\omega t}$, which corresponds to the positive sign before \mathbf{i} in (1.2). If the scattering problem of the time dependence $e^{-i\omega t}$ is considered instead, then the sign before \mathbf{i} in (1.2) should change, and the penalty parameters γ_e in $J(u, v)$ are complex numbers with nonpositive imaginary parts.

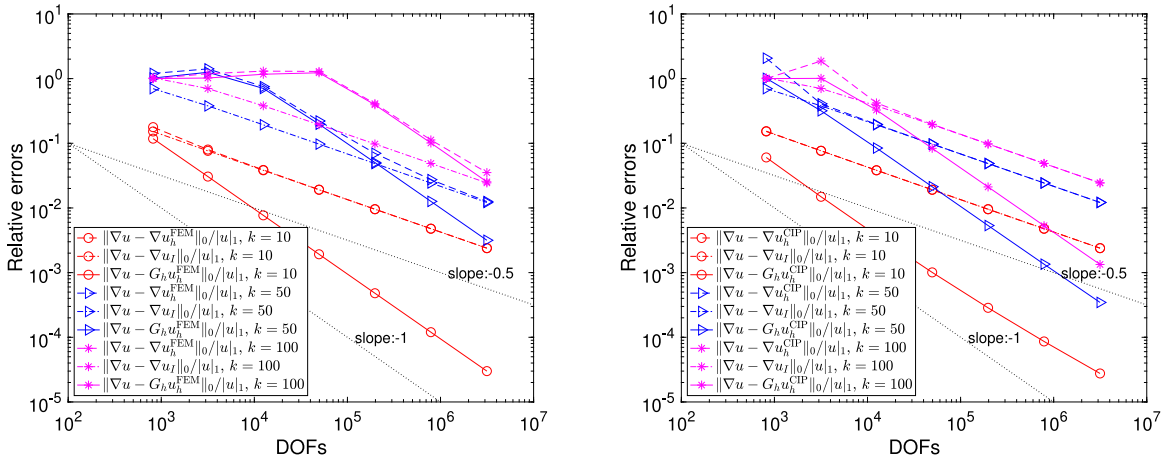


Fig. 3. Left: the relative errors of the FE solution and its recovered gradient versus the total number of degrees of freedom for $k = 10, 50, 100$. Right: the relative errors of the CIPFE solution and its recovered gradient in for $k = 10, 50, 100$. The dotted lines indicate reference slopes.

5. Numerical examples

In this section, we will verify our theoretical results and show the performance of the PPR for FEM and CIPFEM by computing two numerical examples. For the sake of clarity, we denote by u_h^{FEM} the solution of FEM (2.1) and by u_h^{CIP} the solution of CIPFEM (4.23).

5.1. Example 1

We solve the problem (1.1)–(1.2) on the unit regular hexagon with center $(0, 0)$ with $f = \frac{\sin(kr)}{r}$ and g is so chosen that the exact solution is

$$u = \frac{\cos(kr)}{k} - \frac{\cos k + i \sin k}{k(J_0(k) + iJ_1(k))} J_0(kr) \quad (5.1)$$

in polar coordinates, where $J_\nu(z)$ are Bessel functions of the first kind.

For any positive integer m , denote by $\mathcal{T}_{1/m}$ the regular triangulation that consists of $6m^2$ congruent and equilateral triangles of size $h = 1/m$.

From Theorem 4.2, the error of the recovered gradient from the finite element solution in the H^1 -seminorm is bounded by

$$\|G_h u_h - \nabla u\|_0 \leq C_1 k h^{1+\alpha} + C_2 (kh)^2 |\log h|^{\frac{1}{2}} + C_3 k (kh)^2 \quad (5.2)$$

for some constants $C_j, j = 1, 2, 3$, if $k(kh)^2 \leq C_0$. The third term on the right-hand side of (5.2) is the so-called pollution error. We actually have $\alpha \geq 1$ because of the congruent and equilateral triangles in the meshes. In order to reduce the pollution error, we use the CIP-FEM with the following penalty parameters which are obtained by a dispersion analysis on equilateral triangulations (cf. [38]):

$$\gamma_e = -\frac{\sqrt{3}}{24} - \frac{\sqrt{3}}{1728} (kh)^2. \quad (5.3)$$

The left graph in Fig. 3 shows the relative errors of the FE solution and its recovered gradient based on the PPR technique for $k = 10, 50, 100$. It is shown that the error of the recovered gradient converges faster than that of the FE solution for $k = 10$ and that the convergence rate of the recovered gradient appears to be $O(h^2)$. For $k = 50$ and 100 , the relative errors of both the FE solution and its recovered gradient stay around 100% (no-convergence) and finally converge at $O(h)$ and $O(h^2)$, respectively. In addition, the “no-convergence range” increases with k and the decaying points of both the FE solutions and the recovered gradients are the same, which implies the existence of the pollution errors and that their convergence mesh conditions should be the same.

The right graph in Fig. 3 shows the relative errors of the CIPFE solution and its recovered gradient for $k = 10, 50, 100$. We see that the relative error of the CIPFE solution is almost the same as that of the interpolant and the recovered gradient converges at $O(h^2)$ for fixed k , which implies the pollution error is reduced significantly and the PPR technique combining with the interior penalty technique is effective for improving numerical errors. We remark that the numerical tests for the pollution phenomenon of the finite element method have been done largely in the literature. For more details, the readers are referred to [4,8] and references therein.

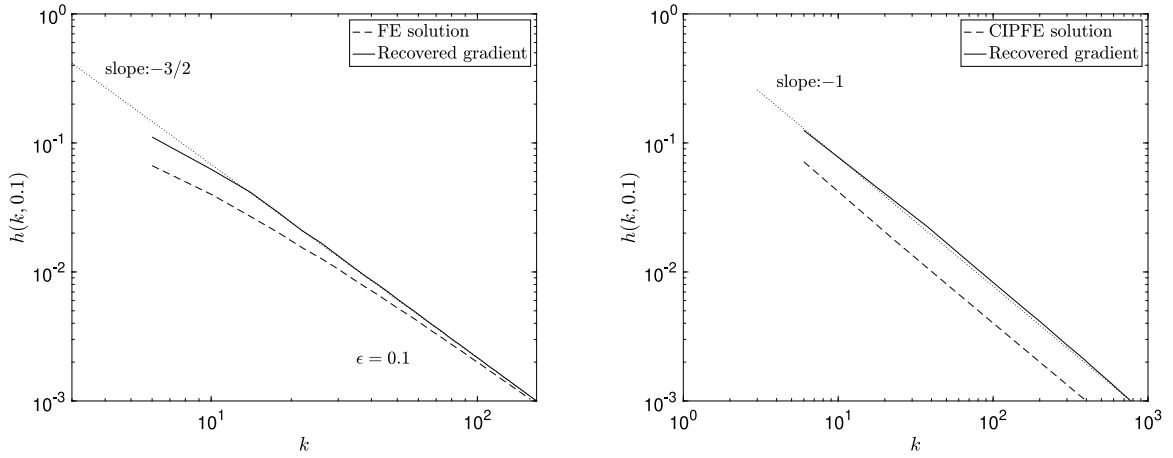


Fig. 4. Left graph: $h(k, 0.1)$ versus k for both the gradient of and the recovered gradient of the FE solution. Right graph: Corresponding plots for the CIPFE solution.

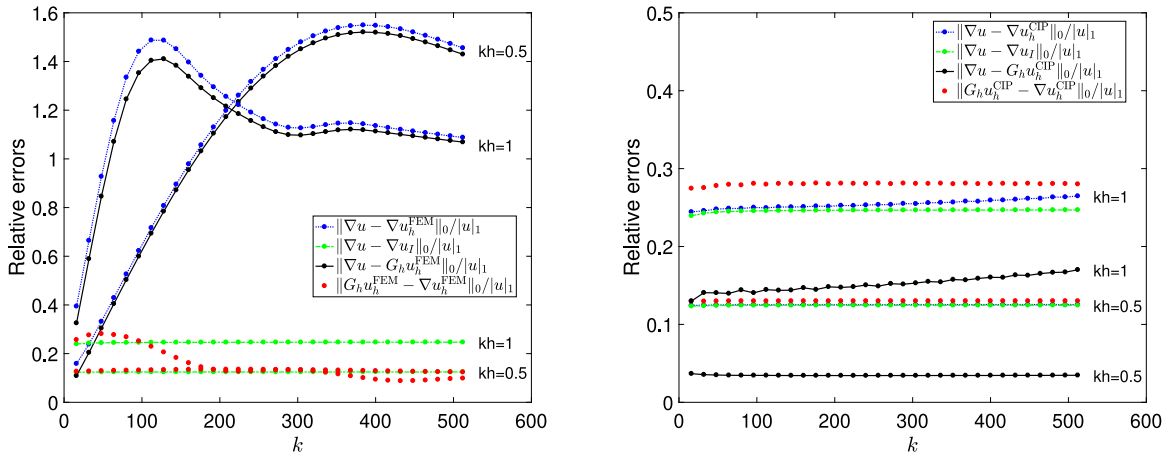


Fig. 5. Left: the relative errors of the finite element solution and its recovered gradient for fixed $kh = 1$ and $kh = 0.5$. Right graph: the relative errors of the CIP finite element solution and its recovered gradient for fixed $kh = 1$ and $kh = 0.5$.

Next we verify more precisely the pollution term in (5.2). To do so, we introduce the definition of the critical mesh size with respect to a given relative tolerance (cf. [7,34]).

Definition 5.1. Given a relative tolerance ε , a wave number k , the critical mesh size $h(k, \varepsilon)$ with respect to the relative tolerance ε is defined by the maximum mesh size such that the H^1 -seminorm relative error of the finite element solution (or the relative error of recovered gradient of the FE solution in the L^2 -norm) is less than or equal to ε .

Clearly, if the pollution terms in (4.16) and (5.2) are of order $k^3 h^2$, then $h(k, \varepsilon)$ should be proportional to $k^{-3/2}$ for k large enough. This is verified by the left graph of Fig. 4. So our theoretical result is sharp with respect to k and h . Furthermore, we plot, in the right graph of Fig. 4, $h(k, 0.1)$ versus k for both the gradient of and the recovered gradient of the CIPFE solution. It is shown that both curves of $h(k, 0.1)$ are almost proportional to k^{-1} which means that the pollution effect does not appear in either ∇u_h or $G_h u_h$ for $h(k, 0.1)$ as small as 0.001. The CIPFE solution is much more accurate than the FE solution and the recovered gradient from the CIPFE solution is even better.

We plot the relative errors of both the FE solution and the CIPFE solution for $k = 1, 2, \dots, 500$ with fixed $kh = 1$ and $kh = 0.5$ in Fig. 5. It is shown in the left graph that both the FE solution and the recovered gradient suffer the pollution effect and that the estimator $\|G_h u_h^{\text{FEM}} - \nabla u_h^{\text{FEM}}\|_0$ approximates actually the interpolation error. However, it can be seen from the right graph that the CIPFE performs much better than the FEM, particularly for fixed $kh = 0.5$ where the relative error of the CIPFE solution is almost same as that of the interpolant, the relative error of recovered gradient is much less than that of the interpolant, and the estimator $\|G_h u_h^{\text{CIP}} - \nabla u_h^{\text{CIP}}\|_0$ approximates the relative error of the CIPFE solution very well.

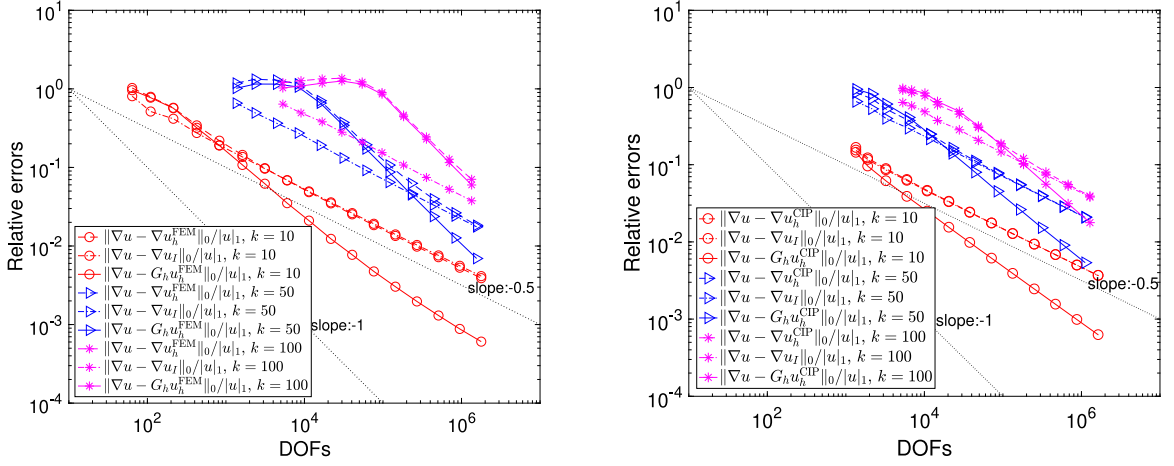


Fig. 6. Left graph: the relative errors of the FE solution and recovered gradient versus the total number of degrees of freedom for $k = 10, 50, 100$. Right graph: the relative errors of the CIPFE solution and recovered gradient for $k = 10, 50, 100$. The dash-dot lines indicate reference slopes in the log-log scale.

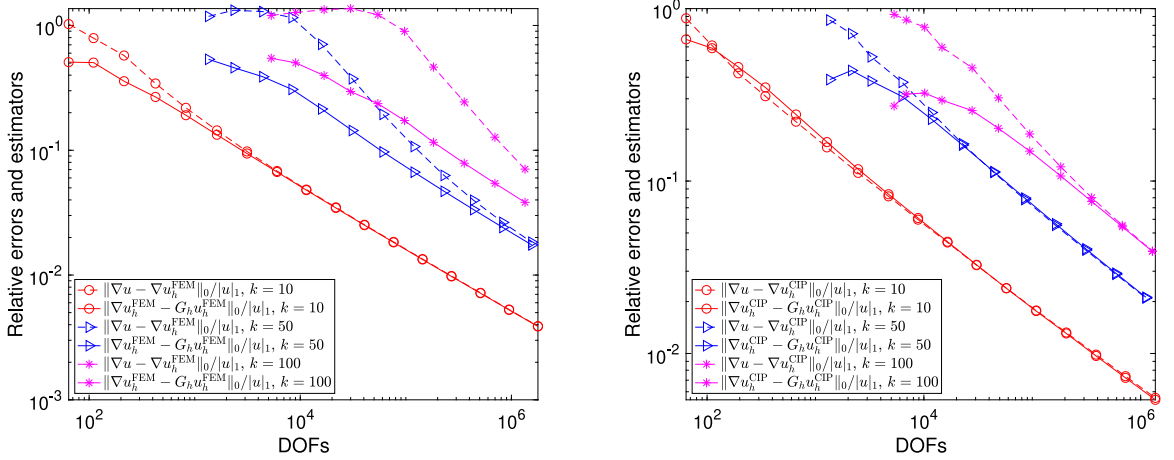


Fig. 7. Left graph: $\|\nabla u - \nabla u_h^{\text{FEM}}\|_0/\|u\|_1$ and $\|G_h u_h^{\text{FEM}} - \nabla u_h^{\text{FEM}}\|_0/\|u\|_1$ versus the total number of degrees of freedom for $k = 10, 50, 100$. Right graph: $\|\nabla u - \nabla u_h^{\text{CIP}}\|_0/\|u\|_1$ and $\|G_h u_h^{\text{CIP}} - \nabla u_h^{\text{CIP}}\|_0/\|u\|_1$ for $k = 10, 50, 100$.

To investigate further the influence of the PPR on the pollution error, we estimate the error between the gradient of the finite element solution and the recovered gradient and prove that this error is controlled by $khC_{u,g}$ (cf. [Theorem 4.3](#)). In [Fig. 5](#), we also depict these errors for $kh = 1$ and $kh = 1/2$, respectively. We see that both of them are dominated by kh , which indicates that both pollution errors are the same.

5.2. Example 2

We solve the Helmholtz problem (1.1)–(1.2) on a L-shaped domain $[-0.5, 0.5]^2 \setminus [0, 0.5] \times [-0.5, 0]$ with the exact solution $J_{\frac{2}{3}}(kr) \sin(\frac{2}{3}\theta)$ in polar coordinates by using the adaptive algorithm based on the PPR (see [\[22\]](#)).

[Fig. 6](#) plots the relative errors of both the FE solution and the CIPFE solution for $k = 10, 50, 100$. Notice that the decay of $\|\nabla u - \nabla u_h^{\text{FEM}}\|_0$ and $\|\nabla u - \nabla u_h^{\text{CIP}}\|_0$ is quasi-optimal and both $\|\nabla u - G_h u_h^{\text{FEM}}\|_0$ and $\|\nabla u - G_h u_h^{\text{CIP}}\|_0$ are superconvergent. By comparing with the relative error of the interpolant, we see that the pollution error is reduced significantly by CIPFEM. [Fig. 7](#) demonstrates asymptotic exactness of the error estimators $\|G_h u_h^{\text{FEM}} - \nabla u_h^{\text{FEM}}\|_0$ and $\|G_h u_h^{\text{CIP}} - \nabla u_h^{\text{CIP}}\|_0$ for the Helmholtz equation on the L-shaped domain, respectively, which shows that the estimator for CIPFEM is a good approximation of the error of the discrete solution in the preasymptotic range while the estimator for FEM is not. [Fig. 8](#) plots the initial mesh and the adaptively refined meshes after 10 adaptive iterations for $k = 10$.

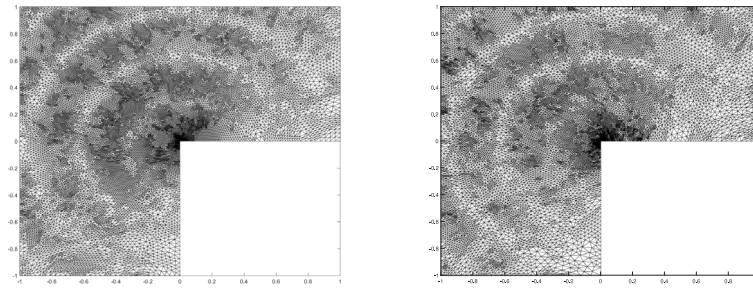


Fig. 8. Left graph: the adaptively refined mesh of 21739 elements after 10 adaptive FEM iterations for $k = 10$. Right graph: the adaptively refined mesh of 16525 elements after 10 adaptive CIPFEM iterations for $k = 10$.

Table 1

Comparisons between the PPR for the Helmholtz equation with high wave number and that for the coercive elliptic equation with Dirichlet boundary condition under the same mesh restriction of (α) .

	Helmholtz	Elliptic
$\ \nabla u - \nabla u_h\ _0$	$O(kh + k^3h^2)$	$O(h)$
$\ \nabla u_h - \nabla u_l\ _0$	$O(kh^{1+\alpha} + (kh)^2 \log h ^{\frac{1}{2}} + k^3h^2)$	$O(h^{1+\alpha})$
$\ \nabla u - G_h u_h\ _0$		
$\ G_h u_h - \nabla u_h\ _0$	$\approx \ \nabla u - \nabla P_h u\ _0 = O(kh)$	$\approx \ \nabla u - \nabla u_h\ _0$

6. Concluding remarks

We have studied superconvergence properties of the linear FEM based on the PPR for the Helmholtz equation with large wave number. Under the assumptions of $k(kh)^2 \leq C_0$ and Condition (α) , we prove that (1) the PPR gradient from the FE solution $(G_h u_h)$ improves the interpolation error but still suffers from the pollution error; (2) $\|G_h u_h - \nabla u_h\|_0$ is not a good estimator of $\|\nabla u - \nabla u_h\|_0$ for h in the preasymptotic range ($k^2 h \gtrsim 1$) while it is actually a good approximation of $\|\nabla u - \nabla P_h u\|_0$; Moreover, our numerical tests show that (3) the PPR combining with the continuous interior penalty technique can improve both the interpolation error and the pollution error; (4) With appropriate penalty parameters, $\|G_h u_h^{\text{CIP}} - \nabla u_h^{\text{CIP}}\|_0$ is a good estimator of $\|\nabla u - \nabla u_h^{\text{CIP}}\|_0$.

Finally, based on our theoretical results (see Theorems 3.1, 4.2, and 4.3) and numerical tests, we make comparisons in Table 1 between the PPR for the Helmholtz equation with high wave number and that for the coercive elliptic equation with Dirichlet boundary condition (see [22,28]).

Acknowledgments

This research work is supported by a Tianhe-2JK computing time award at the Beijing Computational Science Research Center (CSRC). The research of this work was supported in part by the following grants: NSFC 11471031, 91430216, 11525103, 91630309 and 11601026; NASF U1530401; NSF DMS-1419040; Project of Scientific Research Fund of Hunan Provincial Science and Technology Department 2018WK4006; Hunan Provincial Natural Science Foundation of China (NO. 2019JJ50572).

References

- [1] B. Engquist, A. Majda, Radiation boundary conditions for acoustic and elastic wave calculations, *Comm. Pure Appl. Math.* 32 (3) (1979) 313–357.
- [2] J. Douglas Jr., J. Santos, D. Sheen, Approximation of scalar waves in the space-frequency domain, *Math. Models Methods Appl. Sci.* 4 (1994) 509–531.
- [3] M. Ainsworth, Discrete dispersion relation for hp-version finite element approximation at high wave number, *SIAM J. Numer. Anal.* 42 (2004) 553–575.
- [4] I. Babuška, S. Sauter, Is the pollution effect of the FEM avoidable for the Helmholtz equation considering high wave numbers? *SIAM Rev.* 42 (3) (2000) 451–484.
- [5] I. Babuška, F. Ihlenburg, E. Paik, S. Sauter, A generalized finite element method for solving the Helmholtz equation in two dimensions with minimal pollution, *Comput. Methods Appl. Mech. Engrg.* 128 (1995) 325–359.
- [6] L. Zhu, H. Wu, Pre-asymptotic error analysis of CIP-FEM and FEM for Helmholtz equation with high wave number. Part II: *hp* version, *SIAM J. Numer. Anal.* 51 (3) (2013) 1828–1852.
- [7] Y. Du, H. Wu, Preasymptotic error analysis of higher order fem and cip-fem for Helmholtz equation with high wave number, *SIAM J. Numer. Anal.* 53 (2) (2015) 782–804.
- [8] F. Ihlenburg, I. Babuška, Finite element solution of the Helmholtz equation with high wave number. I. The *h*-version of the FEM, *Comput. Math. Appl.* 30 (9) (1995) 9–37.

- [9] A. Aziz, R. Kellogg, A scattering problem for the Helmholtz equation, in: *Advances in Computer Methods for Partial Differential Equations-III*, Vol. 1, 1979, pp. 93–95.
- [10] A. Schatz, An observation concerning Ritz–Galerkin methods with indefinite bilinear forms, *Math. Comp.* 28 (1974) 959–962.
- [11] F. Ihlenburg, I. Babuška, Finite element solution of the Helmholtz equation with high wave number. II. The h - p version of the FEM, *SIAM J. Numer. Anal.* 34 (1) (1997) 315–358.
- [12] J.M. Melenk, S. Sauter, Convergence analysis for finite element discretizations of the Helmholtz equation with Dirichlet-to-Neumann boundary conditions, *Math. Comp.* 79 (272) (2010) 1871–1914.
- [13] J.M. Melenk, S. Sauter, Wavenumber explicit convergence analysis for Galerkin discretizations of the Helmholtz equation, *SIAM J. Numer. Anal.* 49 (3) (2011) 1210–1243.
- [14] E. Burman, L. Zhu, H. Wu, Linear continuous interior penalty finite element method for Helmholtz equation with high wave number: One-dimensional analysis, *Numer. Methods Partial Differential Equations* 32 (2016) 1378–1410.
- [15] J. Melenk, A. Parsania, S. Sauter, General DG-methods for highly indefinite Helmholtz problems, *J. Sci. Comput.* 57 (3) (2013) 536–581.
- [16] X. Feng, H. Wu, Discontinuous Galerkin methods for the Helmholtz equation with large wave numbers, *SIAM J. Numer. Anal.* 47 (4) (2009) 2872–2896.
- [17] X. Feng, H. Wu, hp -Discontinuous Galerkin methods for the Helmholtz equation with large wave number, *Math. Comp.* 80 (276) (2011) 1997–2024.
- [18] Z. Chen, X. Xiang, A source transfer domain decomposition method for Helmholtz equations in unbounded domain, *SIAM J. Numer. Anal.* 51 (2013) 2331–2356.
- [19] Z. Zhang, A. Naga, A new finite element gradient recovery method: Superconvergence property, *SIAM J. Sci. Comput.* 26 (2005) 1192–1213.
- [20] COMSOL Inc., *COMSOL MultiPhysics User'S Guide*, third ed., 2008.
- [21] A. Naga, Z. Zhang, A posteriori error estimates based on the polynomial preserving recovery, *SIAM J. Numer. Anal.* 42 (2004) 1780–1800.
- [22] H. Wu, Z. Zhang, Can we have superconvergent gradient recovery under adaptive meshes? *SIAM J. Numer. Anal.* 45 (2007) 1701–1722.
- [23] R.E. Bank, J. Xu, Asymptotically exact a posteriori error estimators, Part I: Grid with superconvergence, *SIAM J. Numer. Anal.* 41 (2003) 2294–2312.
- [24] A.M. Lakhany, I. Marek, J.R. Whiteman, Superconvergence results on mildly structured triangulations, *Comput. Methods Appl. Mech. Engrg.* 189 (2000) 1–75.
- [25] Z. Zhang, B. Li, Analysis of a class of superconvergence patch recovery techniques for linear and bilinear finite elements, *Numer. Methods Partial Differential Equations* 15 (1999) 151–167.
- [26] J. Douglas Jr., T. Dupont, Interior Penalty Procedures for Elliptic and Parabolic Galerkin Methods, in: *Lecture Notes in Phys.*, vol. 58, Springer-Verlag, Berlin, 1976.
- [27] T. Tang, J. Xu, Topics on adaptive finite element methods, in: *Adaptive Computations: Theory and Algorithms*, Science Press, Beijing, 2007.
- [28] J. Xu, Z. Zhang, Analysis of recovery type a posteriori error estimators for mildly structured grids, *Math. Comp.* 73 (2003) 1139–1152.
- [29] Y. Du, H. Wu, Z. Zhang, Superconvergence analysis of the polynomial preserving recovery for elliptic problems with robin boundary condition, *Mathematica numerica sinica* 40 (2) (2018) 149–170.
- [30] L. Zhu, Y. Du, Pre-asymptotic error analysis of hp -interior penalty discontinuous Galerkin methods for the Helmholtz equation with large wave number, *Comput. Math. Appl.* 70 (2015) 917–933.
- [31] J.H. Bramble, J. Xu, Some estimates for a weighted L^2 projection, *Math. Comp.* 56 (194) (1991) 463–476.
- [32] R.A. Adams, J.J. Fournier, *Sobolev Spaces*, Vol. 140, Academic Press, 2003.
- [33] N. Yan, A. Zhou, Gradient recovery type a posteriori error estimates for finite element approximations on irregular meshes, *Comput. Methods Appl. Mech. Engrg.* 190 (2001) 4289–4299.
- [34] H. Wu, Pre-asymptotic error analysis of CIP-FEM and FEM for Helmholtz equation with high wave number. Part I: Linear version, *IMA J. Numer. Anal.* 34 (2014) 1266–1288.
- [35] I. Babuška, M. Zlámal, Nonconforming elements in the finite element method with penalty, *SIAM J. Numer. Anal.* 10 (5) (1973) 863–875.
- [36] G. Baker, Finite element methods for elliptic equations using nonconforming elements, *Math. Comp.* 31 (1977) 44–59.
- [37] D. Arnold, An interior penalty finite element method with discontinuous elements, *SIAM J. Numer. Anal.* 19 (1982) 742–760.
- [38] C. Han, Dispersion Analysis of the IPFEM for the Helmholtz Equation with High Wave Number on Equilateral Triangular Meshes (Master's thesis), Nanjing University, 2012.